CesrTA LOW EMITTANCE TUNING *

J. P. Shanks, D. Rubin, D. Sagan, Cornell University, Ithaca, NY, 14850, USA

Abstract

Low emittance tuning and characterization of electron cloud phenomena are central to the CesrTA R& D program. A small vertical emittance is required in order to be sensitive to the emittance diluting effects of the electron cloud. We are developing techniques to systematically eliminate optical and alignment errors that are the sources of vertical emittance. Our ability to identify those errors is limited by beam position monitor (BPM) systematics, such as electrode gain errors and BPM misalignments. We report on techniques that we have developed to measure gain variation among the 4 button electrodes on each BPM, and to center BPMs with respect to the adjacent quadrupole. Low emittance also requires that the tune plane be relatively clear of nonlinear coupling resonances associated with sextupoles. We report on tests of a sextupole distribution designed to minimize resonance driving terms. With tuning, we achieve a vertical emittance of $\epsilon_v \sim 19$pm at 2.1 GeV which is near the CesrTA goal of 20pm.

BEAM BASED MEASUREMENT OF BPM ELECTRODE GAINS

The measurement of the transverse position of a beam in a beam position monitor (BPM) depends on the relative response of the BPM electrodes. If there is some variation in gain between electrodes, a systematic error will be introduced into the calculated position. In particular, gain variations can lead to an apparent coupling of horizontal and vertical motions which can confound efforts to minimize the vertical emittance. Gain mapping techniques [1], based on closed orbit data and the ideal electrode response function have proved effective in other machines. We describe an alternative method that relies on turn-by-turn BPM data and a simple approximation of the response function that applies when the electrode geometry is mirror symmetric [2].

In a four button beam position monitor, with buttons arranged symmetrically about the horizontal and vertical axes, it can be shown that

$$B_{+--+} = \frac{c}{I} B_{+-+-} B_{++--} \tag{1}$$

where

$$\begin{aligned} B_{+--+} &\equiv (b_1 - b_2 - b_3 + b_4) \\ B_{+-+-} &\equiv (b_1 - b_2 + b_3 - b_4) \\ B_{++--} &\equiv (b_1 + b_2 - b_3 - b_4) \end{aligned} \tag{2}$$

and $b_1, b_2, \ldots$, etc. are the signals on the buttons, c is a constant that depends on the geometry and I is the beam current. In this notation, buttons 1 and 3 (and 2 and 4) are diagonally opposite. Eqn 2 is valid to second order in the Taylor expansion of the button response about the center of the BPM. In the CESR BPMs, this is an excellent approximation for displacements < 9mm.

Eqn 2 assumes that all of the buttons have the same response function. In practice, the buttons have different gains. Taking this into account gives

$$G \cdot B_{+--+} = \frac{c}{I} (G \cdot B_{+-+-})\,(G \cdot B_{++--}) \tag{3}$$

where

$$G \cdot B_{+--+} \equiv (g_1 b_1 - g_2 b_2 - g_3 b_3 + g_4 b_4), \quad \text{etc.} \tag{4}$$

and g_i is the inverse gain of the i^{th} button. In order to determine the gains, the beam is shaken and the button signals are measured turn-by-turn. Varying g_2, g_3, g_4, and c, a figure of merit χ^2 is minimized with

$$\chi^2 = \sum_{i=1}^{n} \Big((G \cdot B^i_{+--+}) - \frac{c}{I} (G \cdot B^i_{+-+-})(G \cdot B^i_{++--}) \Big)^2 \tag{5}$$

where n is the number of turns. The gains are normalized with respect to button one ($g_1 = 1$). It is convenient to use turn-by-turn data since it can be collected very quickly. The beam is resonantly excited at the horizontal and vertical tunes so that over the course of 1000 turns, a substantial portion of the active region of the BPM is sampled, typically spanning ± 3mm horizontally and vertically.

An example of the data for a typical CESR BPM is shown in Fig. 1. Plotted here is

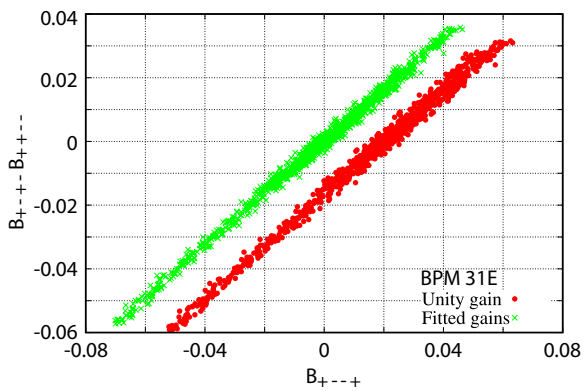

Figure 1: $(B_{+-+-})(B_{++--})$ vs B_{+--+} for resonantly excited beam on 1000 consecutive turns. The red points are raw data assuming equal gain on all buttons. The green points are $(G \cdot B_{+-+-})(G \cdot B_{++--})$ vs $G \cdot B_{+--+}$ where G is the vector of the fitted gains.

* Work supported by the National Science Foundation and by the US Department of Energy under contract numbers PHY-0734867 and DE-FC02-08ER41538.

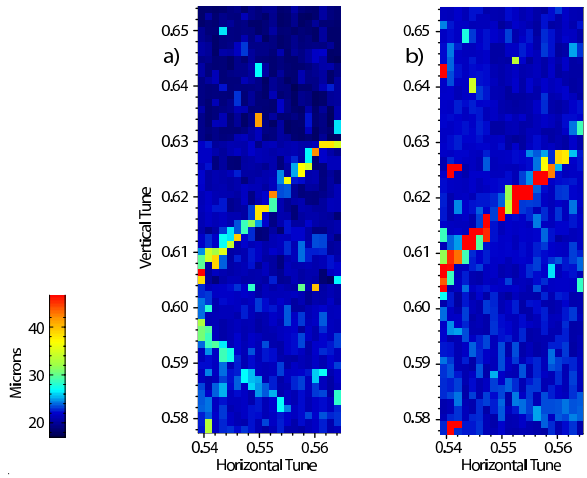

Figure 2: Tune scans over the same tune plane for two sextupole distributions. a): two-family distribution. b): Optimized distribution.

$(B^i_{+-+-})(B^i_{++--})$ vs B^i_{+--+} in red, and $(G \cdot B^i_{+-+-})(G \cdot B^i_{++--})$ vs $G \cdot B^i_{+--+}$ in green where the gains G minimize the χ^2 defined in Equation 5. Note that the green points include $(0, 0)$ as required by Equation 3. Turn by turn data is collected and the gains are fitted for all of the 100 BPMs in CESR in a couple of minutes. Simulations show that the fitting procedure can yield gains with resolution of $< 0.3\%$. After fitting, the four gains for each BPM are normalized so that their average value is unity. The standard deviation of the gains for all 100 CESR BPMs is typically $\sim 4\%$.

TUNE SCANS WITH XBSM

Our X-ray Beam Size Monitor (xBSM) is capable of measuring bunch-by-bunch, turn-by-turn beam sizes for a 14ns bunch spacing [3]. To reduce the effects of turn by turn jitter, the profile is fitted on each turn to a Gaussian and the standard deviations are averaged over 100 turns.

The fast response ($\sim$ 3 seconds) of our xBSM allows us to measure the effects of changing the optics in real-time. We have developed an automated method for scanning the tune plane and measuring the beam size at each point. We use a simple pinhole optics for the xBSM. The pinhole diameter of 16μm, determines the minimum measurable beam size.

Tune scans were performed with two separate sextupole distributions. The first distribution is a simple two-family type. The second is optimized according to the standard prescription to reduce resonance driving terms and increase dynamic aperture [4].

Initial results of tune scans can be seen in Fig. 2. The color scale corresponds to beam size, spanning 18-46 microns. With the optimized sextupole distribution, one of the two visible resonance lines is significantly reduced.

The smallest beam size measured in these tune scans is 18 ± 5 microns, which is near the resolution limit of the pinhole optics. A beam size of 18μm corresponds to an emittance of 19 pm with a substantial uncertainty. 19pm meets the 20pm target for CesrTA.

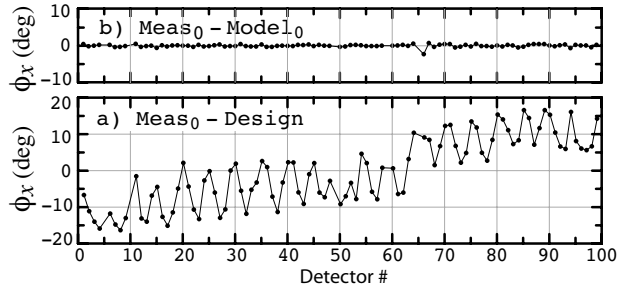

Figure 3: Fit of the baseline Betatron phase data. Only the horizontal phase is shown. All the model quadrupoles are used in the fit. a) Difference between the measured phase and the design phase. b) Difference between measured and model after the fit.

BEAM BASED QUADRUPOLE CENTER MEASUREMENT

The standard beam based technique for measuring the magnetic center of a quadrupole involves measurement of orbit changes with variation of the quadrupole's strength k [5]. One common method for determining the quadrupole center involves taking measurements at various beam positions and then interpolating the results to find the position where the beam orbit does not change with variation of the quadrupole strength. This method has the advantage of not relying on knowledge of the Twiss parameters.

With the present CesrTA BPM system [6], simultaneous orbit, and betatron phase measurements can be taken. This ability makes practical a method whereby the orbit and phase data taken at two quadrupole settings is combined to accurately compute the quadrupole center. This reduces the number of orbit/phase difference measurements that need to be taken and hence reduces the measurement time. The calculation proceeds as follows:

First: Using a software model of the lattice, the model k of all the quadrupole in the model are varied to match the calculated betatron phase to the phase measured at one setting of k of the "target" quadrupole being calibrated. This is called the "base" fit and is denoted with a subscript "0". The measured phase can generally be fit very well as shown in Fig. 3. Only the horizontal phase is shown in the figure. The vertical phase data looks similar. Figure 3a shows the difference between the measured phase and the phase from the theoretical design lattice. The theoretical design lattice is the starting point of the model lattice. Figure 3b shows the difference between the measurement and the model after the fit. The model fits the data quite well. From the model, the beta functions at the quadrupole can be accurately computed.

Second: Starting with the base model, the k of the target quadrupole in the model is varied so that the model phase

most nearly matches the measured phase from the second (non-base) measurement as shown in Fig. 4. As seen in the figure, the phase change is fit very well indicating that the change in strength dk is accurately computed.

Third: Starting from the model fit to the second data set, horizontal and vertical kickers that are superimposed on top of the target quadrupole in the model are used to fit the model orbit difference to the measured orbit difference dx as shown in Fig. 5. The quadrupole center can now be found using the equation

$$dx(s) = (\tilde{x} - x_0(\bar{s}))\, dk\, L \frac{\sqrt{\beta(s)\,\beta(\bar{s})}}{2\,\sin\pi\nu} \cos(|\phi(s) - \phi(\bar{s})| - \pi\nu) \quad (6)$$

where L is the quadrupole length, $\bar{s}$ is the quadrupole location, x_0 is orbit in the base measurement, and the Twiss parameters are evaluated in the non-base configuration.

In the above equation, finite quadrupole length corrections have been ignored. Comparing this to the equation for the orbit deviation due to a kick, the quadrupole center is easily calculated

$$\tilde{x} = \frac{dk}{L\,dk} + x_0(\bar{s}) \quad (7)$$

with similar equations for the vertical plane. Notice that for Eq. 6 to be valid, the orbit at the quadrupole ($x_0(\bar{s})$), as measured at one quadrupole setting, is used in conjunction with the Twiss parameters that exist at the other quadrupole setting. Other parameterizations of the orbit shift are possible [7], but all are equivalent.

CONCLUSION

We have demonstrated a technique for measuring BPM button gains based on resonantly excited turn-by-turn data. Data can be collected and analyzed to give gains for all 100 CESR BPMs in a few minutes.

The ability to simultaneously measure the orbit, along with the betatron phase, provides a fast and accurate method for measuring quadrupole centers and avoids problems with hysteresis and quadrupole calibration inaccuracies. Currently, a single orbit/phase difference takes about

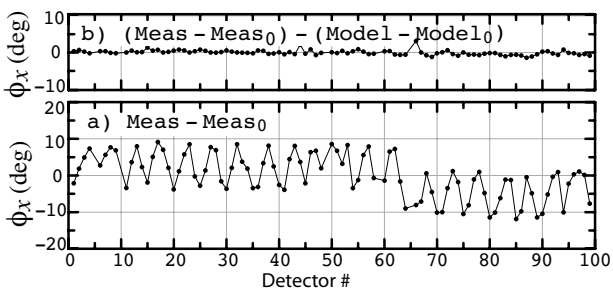

Figure 4: Fit of quadrupole strength change from the betatron phase measurements. a) The phase difference between the base measurement and the second measurement. b) The phase difference from (a) minus the model difference.

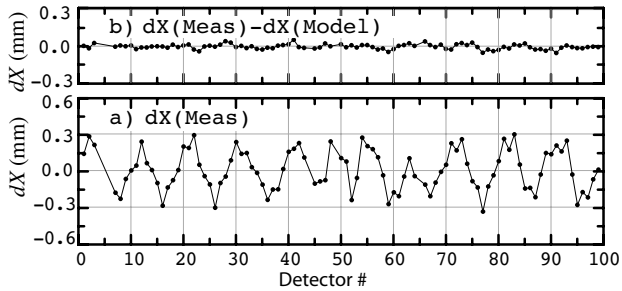

Figure 5: Fit of the orbit change dx due to the change in k. a) The measured orbit change. b) Measured minus fit orbit change.

a minute to measure and analyze. In the future, a further reduction in the measurement time of between a factor of 2 to 4 is possible. Preliminary measurements indicate that the accuracy is below the 100 μm level and more detailed characterizations are planned.

We find that the standard sextupole optimization algorithm reduces the emittance diluting effect of coupling resonances. We have achieved a vertical emittance of $\sim$ 19pm.

ACKNOWLEDGMENT

Thanks to Stu Peck for helpful discussions and help with the benchmarking. Thanks also to Matt Rendina and Mark Palmer for upgrading the BPM system. Finally we thank Dan Peterson for xBSM setup and support.

REFERENCES

[1] K. Satoh and M. Tejima, Proceedings of 1995 Particle Accelerator Conference, Dallas, Texas. p.2482 (1995).

[2] Rubin, D. et. al.,"Beam based measurement of beam position monitor electrode gains", Submitted to Phys. Rev. Accel. and Beams.

[3] D.Peterson et al., "CesrTA X-Ray Beam Size Monitor Operation", Proceedings of the 2010 International Particle Accelerator Conference, Kyoto, Japan

[4] J. Bengtsson, "The Sextupole Scheme for the Swiss Light Source (SLS): And Analytic Approach", Internal Report SLS-TME-TA-1997-0009, PSI 1997

[5] M. Woodley et al., "Beam-Based Alignment at the KEK-ATF Damping Ring", 2004 Europ. Part. Acc. Conf. (2004).

[6] M. Palmer et al., "CESR Beam Position Monitor System Upgrade for CesrTA and CHESS Operations", Proceedings of the 2010 International Particle Accelerator Conference, Kyoto, Japan

[7] A. Wolski and F. Zimmermann, "Closed Orbit Response to Quadrupole Strength Variation", LBNL- 54360, 2004.